Primljen / Received: 21.2.2022.
Ispravljen / Corrected: 14.4.2022.
Prihvaćen / Accepted: 25.4.2022.
Dostupno online / Available online: 10.6.2022.

Effect of perforations and slits on hygrothermal properties of EPS

Authors:

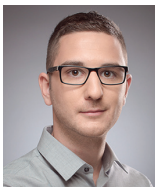

Mergim Gaši, MCE
University of Zagreb
Faculty of Civil Engineering
mergim.gasi@grad.unizg.hr

Assist.Prof. **Bojan Milovanović**, PhD. CE
University of Zagreb
Faculty of Civil Engineering
bojan.milovanovic@grad.unizg.hr
Corresponding author

Prof. **Ivana Banjad Pečur**, PhD. CE
University of Zagreb
Faculty of Civil Engineering
ivana.banjad.pecur@grad.unizg.hr

Marina Bagarić, PhD. CE
University of Zagreb
Faculty of Civil Engineering
marina.bagaric@grad.unizg.hr

Research Paper

Mergim Gaši, Bojan Milovanović, Ivana Banjad Pečur, Marina Bagarić

Effect of perforations and slits on hygrothermal properties of EPS

This paper presents the results of research on the influence of perforation and slits on the water vapour diffusion of expanded polystyrene (EPS) and the influence of the size and number of perforations and slits on the thermal conductivity of EPS board. The research was conducted using numerical models (control volume methods) with varying sample thickness, slit spacing, and depth and diameter of perforations. The numerical model showed that it is possible to obtain up to 42.18 % better water vapour diffusion compared to EPS board without perforation with an increase in thermal conductivity of 9.02 %. Also, the results of this study show that the effective vapour diffusion coefficient depends on the thickness of the perforated EPS samples.

Key words:
numerical model, perforated EPS, heat flow, water vapor diffusion, equivalent thermal conductivity

Prethodno priopćenje

Mergim Gaši, Bojan Milovanović, Ivana Banjad Pečur, Marina Bagarić

Utjecaj perforacija i proreza na higrotermalna svojstva EPS-a

Ovaj rad prikazuje rezultate istraživanja utjecaja perforacija i proreza na difuzivnost vodene pare ekspandiranog polistirena (EPS-a) te utjecaj veličine i broja perforacija i proreza na toplinsku vodljivost ploče EPS-a. Istraživanje je provedeno primjenom numeričkih modela (metode kontrolnih volumena), pri čemu je varirana debljina uzorka, razmak proreza te dubina i promjer perforacija. Numeričkim modelom se pokazalo da je moguće dobiti i do 42,18 % bolju difuzivnost vodene pare u odnosu na EPS ploču bez perforacija uz povećanje toplinske vodljivosti od 9, 02 %. Također, iz rezultata ovog istraživanja vidljivo je da efektivni koeficijent difuzije vodene pare ovisi o debljini perforiranih uzoraka EPS-a.

Ključne riječi:
numerički model, perforirani EPS, toplinski tok, difuzija vodene pare, ekvivalentna toplinska vodljivost

1. Introduction

The European thermal insulation market is characterized by the dominance of two product groups: inorganic fibrous materials and organic foams [1] and, in recent years, the use of these materials, including expanded polystyrene (EPS), has increased sharply due to regulatory changes and co-financing of energy retrofitting of buildings.

When designing a building, one of the first steps is to achieve the required level of thermal protection, in terms of the heat transfer coefficient (U-value), which ranges from about 0.1 W/(m^{2}K) for high energy standards to 0.3 W/(m^{2}K) or more for standard and now common building envelope compositions. The challenge is to achieve such values by choosing the most suitable and economical materials that provide the thinnest possible insulation with the highest level of thermal efficiency [2]. At the same time, and in addition to heat loss, it is necessary to consider the water and moisture transport through the building envelope, material behaviour during temperature fluctuations, as well as the fire behaviour, sound transmission, recovery of the material at the end of its service life, etc. [3].

Among other available materials, EPS is a well-known thermal insulation material used in construction because it has a light but strong foam structure with a low thermal conductivity of 0.030 to 0.050 W/(m K) [4, 5]. In addition, it has a relatively high strength at low density, relatively long service life [6], and requires relatively little maintenance, enabling fast and economical construction [7]. EPS foam is usually composed of several beads, which are usually joined together to form boards. These beads are perfectly spherical, and the cross-section of the bead shows a honeycomb structure with a diameter of 15 μm to 300 μm [8, 9] and a shell with several membranes. This explains the fact that, on the one hand, EPS contains about 98 % air and 2 % polystyrene [7, 8] and, on the other hand, the relatively low water absorption and relatively high water and vapour permeability. The properties of polymer foam are relatively easy to adjust by controlling the pore size, relative density, pore structure, and the use of additives [10, 11].

However, the use of EPS is a major environmental problem and has potentially serious health consequences for humans [12]. It contains substances such as styrene and benzene, which are suspected neurotoxins and carcinogens that could be harmful to humans if released [10]. For styrene, there is convincing relevant information that the substance acts through mechanisms indicating that it is likely to cause cancer in humans [12].

Since polystyrene belongs to a group of organic materials, its behaviour in fire is well known [13]. However, its behaviour in real fire conditions in buildings depends on the conditions in which it is used and on the properties of the material, which may vary depending on whether the polystyrene is manufactured with or without flame retardants.

From a technical point of view, the disadvantage of EPS is thermal expansion. For every 17 °C temperature difference, EPS changes length by about 1 mm/m [14]. Therefore, if the insulation material is (incorrectly) stored at the construction site and has a surface temperature of, for example, 55 °C, its length might be reduced by 2 to 4 mm due to cooling after installation (Table 1). Of course, this can also happen in the opposite direction if the material is installed in winter (direct solar radiation heats up the facade and causes the insulation material to expand).

The coefficients of linear thermal expansion of polymers at room temperature are higher than those of most solid materials because it is a supercooled polymer melt [11]. This large coefficient transfers directly to the expanded state. The authors [11] determined the variation of this property with density and temperature for polystyrene foams and foams in general. When expanded polymers are used in large-scale products, the coefficient of thermal expansion must be carefully considered because of its magnitude compared to that of most non-polymeric materials [11]. The problem occurs in case of possible overheating due to solar radiation, which leads to deformation of EPS boards [15], especially in EPS with the addition of graphite [9, 16], which then leads to the loss of adhesion of facade layers and cracking of the finishing layers of contact facade systems (Figure 1), as well as to an increased heat loss through the voids between insulation boards

Figure 1. Example of cracked finishing layers of ETICS system due to deformation of EPS boards

during the cold period. To relieve the stresses that occur in EPS boards during temperature fluctuations, some EPS manufacturers have developed products with slits throughout the thickness of the EPS board (Figure 2a and Table 1).

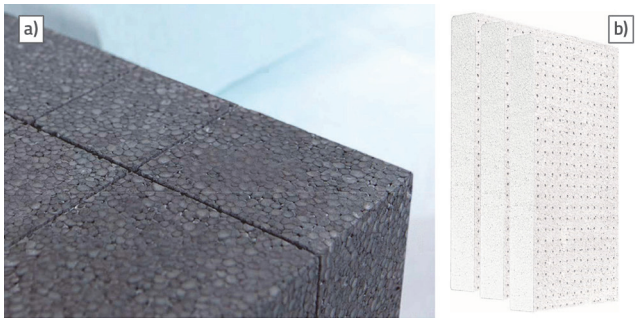

Figure 2. Examples: a) Slits in graphite EPS boards to relieve stresses due to temperature fluctuations; b) EPS boards perforated to reduce water vapour diffusion resistance

Table 1. Linear thermal expansion (dimensional stability) of EPS compared to other thermal insulation materials

Material	Linear thermal expansion $\times 10^{-6}$ [K^{-1}]	Expansion of the 1 m long board at ΔT = 50 °C [mm]
White EPS	50 - 70 [17.18] 63 [19] 80 [20]	2.5 - 3.5 3.15 4.0
Graphite EPS	65 [21] 60 - 80 [22]	3.25 3.0 - 4.0
XPS	80 [18] 63 [19]	4.0 3.15
PUR	100 [18] 30 - 80 [24]	5.0 1.5 - 4.0
PIR	120 [18] 30 - 80 [23] 54 - 140 [19]	6.0 1.5 - 4.0 2.7 - 7.0
Mineral wool	5.5 [18] 9 - 14 [19]	0.28 0.45 - 0.7

In case of a cut and perforated EPS board, the coefficient of linear thermal expansion is the same as for the material out of which the EPS board is made (white or graphite EPS), while the relative expansion or shortening of the board is controlled by making slits.

In addition, the vapour diffusion resistance factor μ (-) is one of the most important properties for water vapour transport through the building envelope in terms of hygrothermal behaviour. It therefore defines the ability of a material to leak, or conversely, to prevent the transport of water vapour through the material, and is determined by the dry glass method according to HRN EN 12086 [24]. For still air, the μ-value is 1. The higher the μ-value, the greater the resistance of the material to the passage of water vapour.

Vapour diffusion is the movement of water vapour molecules through porous materials (e.g., wood, insulation, concrete, etc.) driven by the difference in partial vapour pressure. Differences in partial vapour pressure result from differences in air temperature and vapour contained in the air. Diffusion of water vapour through a building element always occurs from a high to a low partial pressure of water vapour, i.e. mostly from the warm to the cold side, since warm air can store more water vapour than cold air.

In cold climates, this means that water vapour is transported mainly from the heated indoor space to the colder outdoor spaces, while in hot climates the direction of water vapour transport is reversed and occurs mainly from the warm, humid outdoor space to the air-conditioned indoor space. The direction of water vapour transport can also be reversed when the sun heats up damp, absorbent wall coverings and masonry, forcing the water vapour inward.

The increasingly stringent regulatory requirements in the field of energy efficiency require an increase in the thickness of thermal insulation. The added thickness of insulation and the changes in water vapour flow that occur after insulation is added require rethinking water vapour transport and condensation control, as well as increased moisture content of the material within the building elements.

The varying vapour permeability of various insulating materials, membranes, and other building materials adds considerable complexity to the design and construction of building elements. Some insulation materials, such as mineral wool, are vapour permeable, while others, such as extruded polystyrene (XPS), expanded polystyrene (EPS), polyisocyanurate (PIR), and polyurethane (PUR), are relatively impermeable to vapour (Table 2).

Table 2. Diffusion of water vapour through EPS compared to other thermal insulation materials

Material	Density ρ [kg/m^3]	Water vapor diffusion coefficient μ [-]
White EPS	15 [28]	20-40 [28]
	20-25 [28]	30-70 [28]
	30-35 [28]	40-100 [28]
	10-50 [4]	20-100 [4]
	>15 [20]	35+2.1*(ρ-15) [20]
Graphite EPS	15-18 [22]	20-70 [22]
Cut (slitted EPS)	15 [29] 25 [30]	45 [29. 31] 40-100 [30]
Perforated EPS	15-18 [30] 15-18 [32] 20 [29] 15-20 [33]	7 [34] 8 [30] 10 [32] 10 [29] 10-30 [33]
XPS	20-65 [4]	80-250 [4]
	>20 [20]	114+3.42*(ρ-20) [208]
PUR	34.03 [35]	56 [35]
	28-55 [4]	40/200 [4]
PIR	26.5 [36]	51.5 [36]
Mineral wool	10-200 [4] 39 [37]	1 [4] 2 [37]

The choice of a particular arrangement of material layers in the building element, and the vapour permeability of these layers, control the transport of water vapour, and, in the case of EPS, water vapour diffusion is the dominant mechanism [25]. The control of water vapour diffusion is one of the ways to control the occurrence of condensation and the location of the dew point within the wall.

For example, the patent DE A110007774 [26] discloses a thermal insulation board made of polystyrene (EPS / XPS) or polyurethane (PUR) with a water vapour diffusion coefficient $\mu < 10$ [26, 27]. To achieve this value, the EPS board must have small diameter holes (perforations) distributed over the surface. The hole diameter is between 1 and 5 mm, preferably between 1.5 and 3 mm, and the distance between the holes (perforations) is between 10 and 100 mm, preferably 50 – 70 mm [26, 27], so that a low thermal conductivity of EPS boards can be obtained. For making the perforations, it is suggested to drill the finished boards with hot needles to obtain a welded and thus smooth surface on the perforated area, which should be favourable for the transport of water vapour [26, 27].

In terms of building physics, physical advantages of mineral fibre insulation in external thermal insulation composite systems (ETICS) in Central Europe result primarily from the diffusion openness of the material. If we consider the drying of wall structures with different ETICS systems, we can see that, when rigid foam insulation (EPS) is used, the diffusion flow, which is important for exterior drying, is reduced due to the relatively higher diffusion resistance of EPS itself as thermal insulation [38]. Therefore, some manufacturers have been developing polystyrene-based products with a lower coefficient of water vapour diffusion resistance. At the same time, the manufacturers declare the values of thermal conductivity of the boards as the same as for classical EPS boards (depending on whether it is graphite or white EPS) [29, 32, 33]. The widespread use of EPS as thermal insulation in construction requires a sustained improvement in the hygrothermal properties of conventional building products. Therefore, some progress is being made in reducing thermal conductivity, for example, by adding graphite [8, 16] and, in the case of reducing resistance to water vapour diffusion, by perforation or slots (slits) on the boards that allow stress relief with temperature changes.

When introducing various technological changes, it is important to understand the physical consequences that such changes cause. A better understanding can be achieved through the use of numerical modelling at the material level to confirm the direction of product development. Numerical modelling can enable engineers to develop new materials and encourage industry stakeholders to optimize more efficiently the manufacturing cost of these products, all aimed at ensuring better control of the heat and moisture transport through the building envelope.

Therefore, the goal of this research is to use numerical models to draw conclusions that can answer the following two questions:

- What influence do perforations and slits have on the water vapour diffusivity of EPS?
- Do the size and number of perforations and slits influence thermal properties of EPS boards?

Table 3. Simulation cases ID

No.	ST [cm]	SS [cm]	DP [cm]	PD [mm]	Case ID
1	10	10	5	2	DU10_RS10_DP5_PP2
2	10	10	5	5	DU10_RS10_DP5_PP5
3	10	10	10	2	DU10_RS10_DP10_PP2
4	10	10	10	5	DU10_RS10_DP10_PP5
5	10	20	5	2	DU10_RS20_DP5_PP2
6	10	20	5	5	DU10_RS20_DP5_PP5
7	10	20	10	2	DU10_RS20_DP10_PP2
8	10	20	10	5	DU10_RS20_DP10_PP5
9	20	10	5	2	DU20_RS10_DP5_PP2
10	20	10	5	5	DU20_RS10_DP5_PP5
11	20	10	20	2	DU20_RS10_DP20_PP2
12	20	10	20	5	DU20_RS10_DP20_PP5
13	20	20	5	2	DU20_RS20_DP5_PP2
14	20	20	5	5	DU20_RS20_DP5_PP5
15	20	20	20	2	DU20_RS20_DP20_PP2
16	20	20	20	5	DU20_RS20_DP20_PP5
17	30	10	5	2	DU30_RS10_DP5_PP2
18	30	10	5	5	DU30_RS10_DP5_PP5
19	30	10	30	2	DU30_RS10_DP30_PP2
20	30	10	30	5	DU30_RS10_DP30_PP5
21	30	20	5	2	DU30_RS20_DP5_PP2
22	30	20	5	5	DU30_RS20_DP5_PP5
23	30	20	30	2	DU30_RS20_DP30_PP2
24	30	20	30	5	DU30_RS20_DP30_PP5

2. Research methodology

The research was conducted using numerical methods to simulate the transport of heat and water vapour through EPS panels. Numerical calculation of the heat and water vapour conduction was performed according to HRN EN ISO 10211 (Thermal bridges in building construction - Heat flows and surface temperatures - Detailed calculations) [39] and HRN EN ISO 13788 (Hygrothermal performance of building components and building elements - Internal surface temperature to avoid critical surface humidity and interstitial condensation - Calculation methods) [40]. The process of heat exchange through the interfaces is assumed to be adiabatic - there is no exchange of heat with the environment through the interface. Boundary conditions and equivalent thermal properties of air were calculated according to HRN EN ISO 6946 (Building components and building elements - Thermal resistance and thermal transmittance - Calculation methods) [41] and HRN EN ISO 10077-2 (Thermal performance of windows, doors and shutters - Calculation of thermal transmittance - Part 2: Numerical method for frames) [42]. The numerical calculation was performed using AnTherm [43], a computer program specialized in the calculation of thermal bridges / heat transfer and water vapour diffusion.
The aim of this study is to quantify the influence of perforations in expanded polystyrene (EPS) boards on their hygrothermal properties, i.e., the heat flow and water vapour transfer, using numerical simulations. Twenty-four different combinations were analysed in order to take into account different arrangements and sizes of the perforations and different sample thicknesses (Table 3). The following parameters were varied throughout the study:

- Sample thickness (ST) of 10, 20 and 30 cm.
- Slit spacing (SS) of 10 and 20 cm.
- Depth of perforation (DP) of 5 cm and throughout the whole thickness of the sample (10, 20 and 30 cm).
- Perforation diameter (PD) of 2 and 5 mm.

The dimensions of the EPS boards considered in this study are 1500 × 500 mm, and the thickness of the boards ranges from 100 to 300 mm. The width of the slit was assumed to be 2 mm in all cases.

3. Theoretical background

3.1. Heat conduction

In the physical sense, the property of a material called "thermal conductivity" is the ratio of the vector "heat flow rate" in the material to the vector "temperature gradient" at the same location in the material [20]. For isotropic materials, this ratio is scalar, and the heat conduction through a homogeneous material is defined by Fourier's law [44]:

$$\vec{q} = -\lambda \cdot grad\, T \tag{1}$$

where T is the temperature in the coordinate (x, y, z), and λ is the thermal conductivity of the material.

If equation (1) is established for the final volume $dx \times dy \times dz$, then the sum of the heat flows through the surfaces describing the volume is equal to the heat generated in that element.

$$Q_x = -\lambda \cdot dy \cdot dz \cdot \frac{\Delta T}{dx}$$

$$Q_y = -\lambda \cdot dx \cdot dz \cdot \frac{\Delta T}{dy} \tag{2}$$

$$Q_z = -\lambda \cdot dx \cdot dy \cdot \frac{\Delta T}{dz}$$

$$\sum_{i=x,y,z} Q_i = Q_{gen}$$

In case there is no heat generation (e.g., underfloor heating) then the member $Q_{gen} = 0$.
By outputting the equations for each final volume and solving the system of equations, the unknown temperatures are obtained. For the analogy of heat conduction and water vapour diffusion, equation (1) can be written as follows:

$$\vec{q} = -\lambda \cdot \Delta T \quad W/m^2 \tag{3}$$

3.2. Equivalent diffusion of water vapour

The term "equivalent" emphasizes that the so-called diffusion in porous materials combines molecular and frictional diffusion, surface flow, and water transfer in small pores filled with capillary condensation [44]. Since the vapour phase dominates, this complex reality is described by Fick's diffusion law. When convection is negligible, this type of diffusion provides a model for estimating the transfer of "vapour" through building elements. Of course, the absence of convection would mean that the building element contains no air layers, no cracks, etc., i.e., the building envelope is assumed to be airtight. Since EPS has a very low air permeability and is a material without open pores, it can be assumed that the diffusion of water vapour through EPS is defined by Fick's first law:

$$\vec{d} = -\delta \cdot grad\, c \tag{4}$$

Where c is the concentration of water vapour, and δ is the coefficient of proportionality (diffusion coefficient).
The diffusion coefficient δ for air at an air pressure of 1 atm (101325 Pa) and an air temperature of 10 °C is equal to:

$$\delta = 2{,}36 \cdot 10^{-5} \quad m^2/s \tag{5}$$

If vapour density R_D is used as a measure of water vapour concentration, and assuming the validity of Dalton's law [44], equation (4) for air can be written as follows:

$$\vec{d} = -\frac{\delta}{R_D \cdot T} \cdot grad\, p_D \tag{6}$$

Where R_D is the gas constant for water vapour, T is the absolute temperature, and p_D is the partial density of water vapour (partial vapour pressure).
For a temperature of 10 °C (283,15 K) and the gas constant R_D = 461,5 J/kgK, the coefficient of proportionality d/($R_D \cdot T$) is [45]:

$$\frac{\delta}{R_D \cdot T} = 1{,}806 \cdot 10^{-10}\ s = 6{,}502 \cdot 10^{-7}\ h \quad (7)$$

In the case of water vapour diffusion through a homogeneous layer of air with thickness d, equation (4) can be formulated as:

$$\vec{d} = -\frac{6{,}502 \cdot 10^{-7}}{d} \Delta p_D \quad \text{kgm}^2\text{h}^{-1} \quad (8)$$

By analogy with heat conduction and thermal resistance increasing with thickness, equation (8) can be written such that diffusion resistance increases with an increase in layer thickness (at a pressure of 101325 Pa and a temperature of 283.15 K) [45]:

$$\frac{d}{6{,}502 \cdot 10^{-7}} = 1{,}538 \cdot 10^{6} \cdot \text{d} \quad \text{mh}^{-1} \quad (9)$$

That is, in the software package AnTherm [43] and in the standard ÖNORM B 8110-2, the design resistance to water vapour diffusion s was assumed to be:

$$s = 1{,}5 \cdot 10^{6} \cdot \text{d} \quad \text{mh}^{-1} \quad (10)$$

For building materials, water vapour diffusion is defined by the dimensionless water vapour diffusion resistance factor (μ-value). The μ factor indicates how much greater the water vapour diffusion resistance of a homogeneous building material layer is compared to an air layer of the same thickness. In the case of building materials, equation (5) can thus be better expressed as:

$$\vec{d} = -\frac{10^{-6}}{1{,}5 \cdot \mu \cdot d} \cdot \Delta p_D \quad \text{kgm}^2\text{h}^{-1} \quad (11)$$

The model of heat conduction and the water vapour diffusion model are taken to be analogous in this study, the only difference being the replacement of thermal conductivity λ with 10^{-6}/(1,5·μ·d) and the replacement of temperature differences ΔT with the difference of partial pressures of water vapour Dp_D. In the case of water vapour diffusion, the resistance of the water vapour transport from the environment to the surface of the element is neglected in the model. The standard HRN EN ISO 13788 [40] defines the conductivity coefficient of water vapour diffusion as being equal to 2 · 10^{-10} kg/(*Pa*·*m*·*s*). By converting this coefficient into units of measurement used in AnTherm, a coefficient of 1.3888 is obtained, and so a coefficient of 1.5 otherwise used in AnTherm is replaced with a coefficient of 1.3888 [45].

4. Research metrics

4.1. Minimum surface temperature $\Theta_{si,\,min}$

The minimum surface temperature on the internal surface $\Theta_{si,\,min}$ (°C) represents the place with the highest risk of water vapour condensation and the formation of fungi and mould.

4.2. Temperature factor f_{Rsi}

The temperature factor on the internal surface f_{Rsi} is a dimensionless factor that shows the risk of surface condensation. The factor f_{Rsi} is calculated as follows [44]:

$$f_{Rsi,\min} = \frac{\Theta_{si,\min} - \Theta_e}{\Theta_i - \Theta_e} \quad (12)$$

The values of the factor f_{Rsi} range from 0 to 1:
$f_{Rsi} \approx 0$: the internal surface temperature is close to the outdoor air temperature and the risk of surface condensation is high.
$f_{Rsi} \approx 1$: the internal surface temperature is close to the indoor air temperature and the risk of condensation is low.
The coefficient f_{Rsi} is calculated based on the minimum internal surface temperature $\Theta_{si,min}$.

4.3. Thermal coupling coefficient $L_{3D,\,therm}$

The total heat flow in Watts between two selected environments for the unit temperature difference obtained by 3D numerical calculation is called the thermal coupling coefficient ($L_{3D,\,therm}$) [37].

$$L_{3D,therm} = \frac{\Phi_T}{T_i - T_j} W/K \quad (13)$$

Where F_T is the total heat flow between environments "i" and "j", while T_i and T_j are temperatures of environments "i" and "j".

4.4. Diffusion coupling coefficient $L_{3D,diff}$

As explained in Section 3.2, the calculation of water vapour diffusion and heat conduction are two equivalent calculations in terms of numerical calculation. They differ only in the proportionality coefficient, which is equal to λ in the case of heat conduction (Equation 3), while it is equal to 10^{-6}/(1,5·μ· d) in the case of water vapour diffusion (Equation 11). Since in both cases it is a linear system for which the superposition principle applies, the procedure for calculating the diffusion coupling coefficient is equivalent to the calculation of the thermal coupling coefficient given in the standard HRN EN ISO 10211 [39].

The diffusion coupling coefficient ($L_{3D,\ diff}$) is equal to the total water vapour flow in milligrams per hour between two selected environments at an air pressure difference of 1 Pa, determined by 3D numerical calculation.

$$L_{3D,dif} = \frac{\Phi_D}{p_i - p_j} \quad \text{mg/(Pa·h)} \tag{14}$$

Where Φ_D is the total water vapour flow between environments "i" and "j", while p_i and p_j are partial vapour pressures of individual environments.

5. Numerical calculations

The numerical calculation was performed using the computer program AnTherm [43], which specializes in the calculation of thermal bridges / heat transfer and water vapour diffusion.
The numerical calculation in AnTherm is based on the method of control volumes (MCV), i.e., the mesh of control volumes is such that it must be prismatic. The surfaces of each control volume must be in complete contact, and the heat and water vapour flows are calculated for them according to Kirchhoff's second diffusion law, from which the unknown quantities are determined:
- temperatures
- partial water vapour pressures.

According to the standard HRN EN ISO 10211 [39], the mesh of control volumes is determined in such a way that the following condition is satisfied in two successive numerical calculations with two different meshes:

$$L_{3D}^{i+1} - L_{3D}^{i} < 1\,\% \tag{15}$$

where "i+1" and "i" are two consecutive numerical calculations.

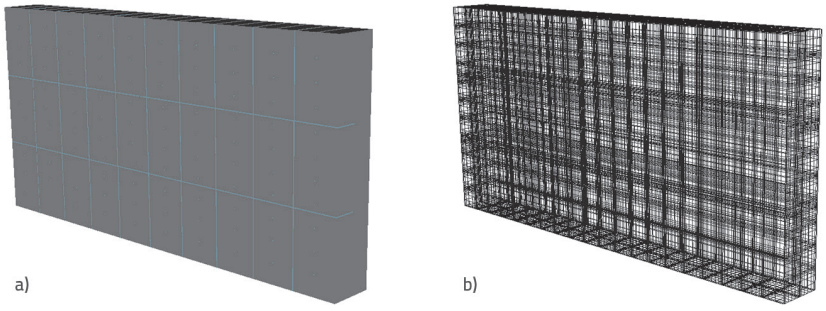

Figure 3. Example of a simulated EPS board: a) geometric model, b) control volumes mesh

Table 5. Boundary conditions

Boundary conditions	Surface heat transfer coefficient h [W/(m² K)]	Thermal resistance R [(m² K)/W]	Temperature T [°C]	Relative humidity RH [%]
Exterior	25.0	0.04	-10.0	80.0
Interior	7.69	0.13	20.0	53.0

The mesh size of the control volumes is defined in AnTherm in the range between 2 and 50 mm, with a 2 mm increment between the two mesh thickenings. Figure 3 shows an example of a control volume mesh. In this study, the sample size of EPS is the same for all 24 combinations, namely 1500 × 500 mm.

5.1. Material properties

Since the literature review revealed that the vapour diffusion coefficient for EPS depends on the specific products of each manufacturer (Table 2), in this study, the material properties were taken from the Technical regulation on energy economy and heat retention in buildings (TPRUETZZ) [5], and calculated according to the standards HRN EN ISO 10077-2 and HRN EN ISO 6946 (Table 4).

Table 4. Material properties

Material	λ [W/(m K)]	μ [--]	Source
EPS	0.032	40.0	TPRUETZZ [5]
Air	0.250*	1.0	HRN EN ISO 10077-2 [42]/ HRN EN ISO 6946 [41]
Note (*): The thermal conductivity of air varies with the dimensions of the air layer (cavity) and its exposure to the outside air.			

5.2. Boundary conditions

Boundary conditions were determined according to HRN EN ISO 10211 [39] and HRN EN ISO 6946 [41] (Table 5).

6. Results

Figure 4 shows the distribution of temperature and partial pressure of water vapour for the ST10_SS10_DP5_PD2 combination, from which the values of minimum internal surface temperatures and relative humidity per element cross-section are calculated. For all other combinations, the results of the numerical calculations are analogous, and are not presented here for the sake of brevity. It can be seen that there is an increased heat flow through the perforations and slits resulting in a lower temperature in the temperature field at the perforation and slit locations (Figure 4a). Similarly, there is a decreased partial pressure of the water vapour at the perforation and slit locations (Figure 4b), indicating that there is an increased diffusion flow of the water vapour at these locations. Figure 4c) shows a magnified view of the temperature distribution at a depth of 50 mm extending over a mesh of control volumes.

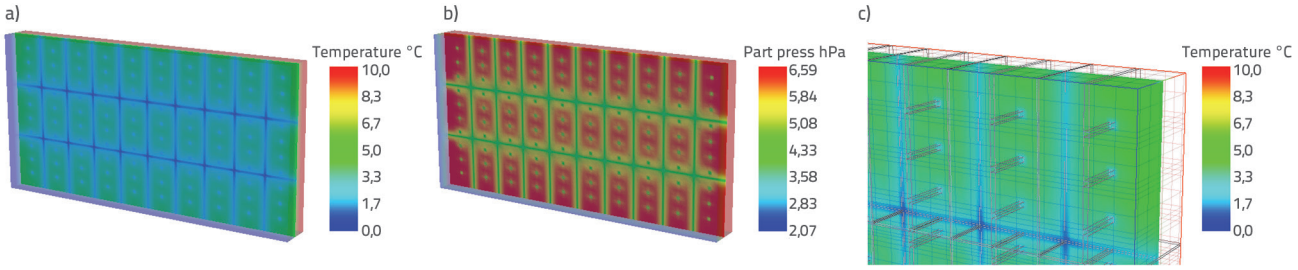

Figure 4. Calculation results: a) temperature; b) partial vapour pressure; c) temperature near perforations (enlarged view)

The results of the calculation are the minimum internal surface temperatures $\Theta_{si,\,min}$, the temperature factors on the internal surface f_{Rsi} and the coefficients of thermal and diffusion coupling L3D (Table 6 and Table 7).

Also, the increase of heat losses and water vapour diffusion flow (Table 6) is presented in comparison with the reference cases for EPS without slits and perforations (Table 7):

$$\Delta L_{3D}^{1} = \frac{\left(L_{3D,therm} - L_{3D,therm,ref}\right)\Big|_{d=10,20,30}}{L_{3D,therm,ref}} \tag{16}$$

$$\Delta L_{3D}^{2} = \frac{\left(L_{3D,diff} - L_{3D,diff,ref}\right)\Big|_{d=10,20,30}}{L_{3D,diff,ref}} \tag{17}$$

Table 6. Results of numerical calculations

No.	Case ID	$\Theta_{si.min}$ [°C]	f_{Rsi} [-]	$L_{3D.therm}$ [W/K]	$L_{3D.diff}$ [mg/(Pa h)]	ΔL_{3D}^{1} [%]	ΔL_{3D}^{2} [%]
1	DU10_RS10_DP5_PP2	18.74	0.96	0.161985	0.111911	-6.59	24.35
2	DU10_RS10_DP5_PP5	18.74	0.96	0.163022	0.113485	-7.27	26.09
3	DU10_RS10_DP10_PP2	17.94	0.93	0.162410	0.114030	-6.87	26.70
4	DU10_RS10_DP10_PP5	16.96	0.90	0.165690	0.127966	-9.02	42.18
5	DU10_RS20_DP5_PP2	18.75	0.96	0.158351	0.104487	-4.19	16.10
6	DU10_RS20_DP5_PP5	18.74	0.96	0.159922	0.107966	-5.23	19.96
7	DU10_RS20_DP10_PP2	17.98	0.93	0.158766	0.106458	-4.47	18.29
8	DU10_RS20_DP10_PP5	17.34	0.91	0.162538	0.121422	-6.95	34.91
9	DU20_RS10_DP5_PP2	19.39	0.98	0.080386	0.049610	-3.14	10.24
10	DU20_RS10_DP5_PP5	19.39	0.98	0.080742	0.050168	-3.59	11.48
11	DU20_RS10_DP20_PP2	18.82	0.96	0.080711	0.050897	-3.55	13.10
12	DU20_RS10_DP20_PP5	18.47	0.95	0.082776	0.058405	-6.20	29.79
13	DU20_RS20_DP5_PP2	19.40	0.98	0.079514	0.048145	-2.02	6.99
14	DU20_RS20_DP5_PP5	19.40	0.98	0.079889	0.048820	-2.50	8.49
15	DU20_RS20_DP20_PP2	18.83	0.96	0.079835	0.049385	-2.43	9.74
16	DU20_RS20_DP20_PP5	18.48	0.95	0.081896	0.056833	-5.07	26.30
17	DU30_RS10_DP5_PP2	19.60	0.99	0.053504	0.031981	-2.09	6.60
18	DU30_RS10_DP5_PP5	19.60	0.99	0.053662	0.032212	-2.39	7.37
19	DU30_RS10_DP30_PP2	19.22	0.97	0.053746	0.032870	-2.55	9.57
20	DU30_RS10_DP30_PP5	18.98	0.97	0.055172	0.037850	-5.27	26.17
21	DU30_RS20_DP5_PP2	19.60	0.99	0.053117	0.031365	-1.35	4.55
22	DU30_RS20_DP5_PP5	19.60	0.99	0.053284	0.031650	-1.67	5.50
23	DU30_RS20_DP30_PP2	19.22	0.97	0.053356	0.032232	-1.80	7.44
24	DU30_RS20_DP30_PP5	18.99	0.97	0.054780	0.037183	-4.52	23.94

Legend:

Best case; Medium good case; Worst case

Table 7. Calculation results for EPS without slits and perforations

Reference models	$\Theta_{si.min}$ [°C]	f_{Rsi} [--]	$L_{3D.therm.ref}$ [W/K]	$L_{3D.diff.ref}$ [mg/(Pa h)]
ST10	18.86	0.96	0.151976	0.090000
ST20	19.42	0.98	0.077942	0.045000
ST30	19.61	0.99	0.052411	0.030000

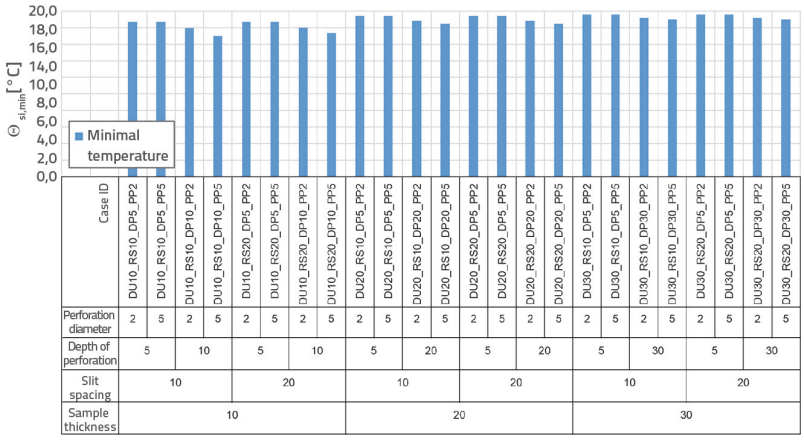

Figure 5. Minimum internal surface temperatures

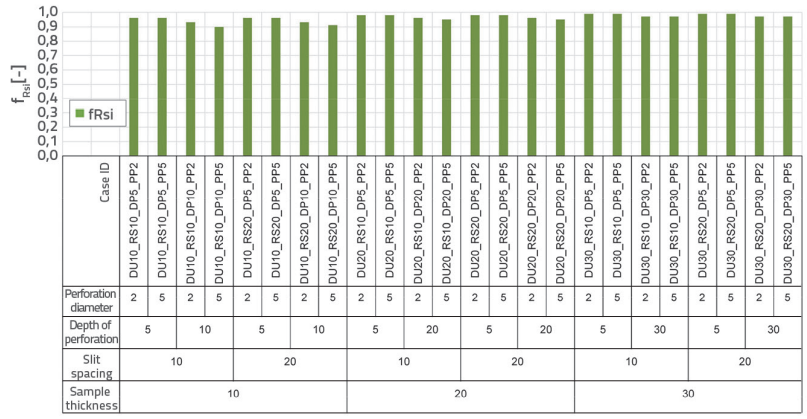

Figure 6. Temperature factors on the inner surface

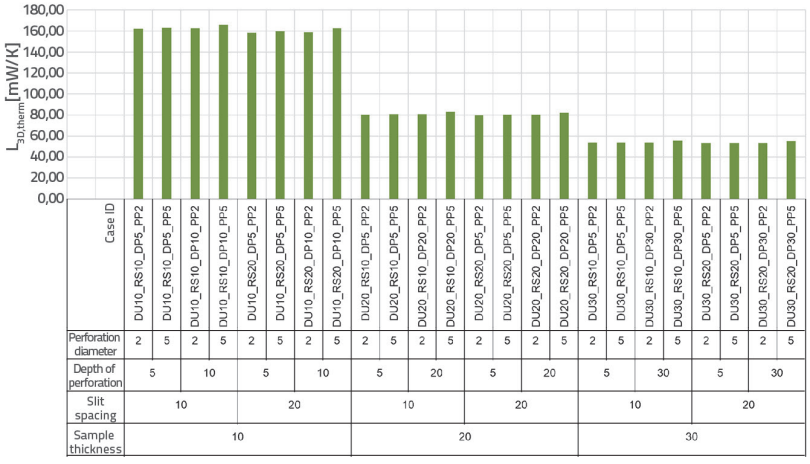

Figure 7. Thermal coupling coefficients

Figures 5 to 10 provide a graphical representation of calculation results for all 24 combinations. The results were grouped by sample thickness (10 to 30 cm), slit spacing (slots) (10 and 20 cm), perforation depth (5 cm and total sample depth), and perforation diameter (2 and 5 mm).

Figure 5 and Figure 6 show the minimum internal surface temperatures and the corresponding temperature factors. As expected, the calculation results suggest that the internal surface temperatures increase with an increase in sample thickness and perforation depth (Figure 5). Thus, a surface temperature difference amounts to 1.78 °C (for perforations of 5 and 10 cm in depth with a diameter of 5 mm for a 10 cm thick sample with a 10 cm slit spacing), and to 0.62 °C (for perforations of 5 and 30 cm in depth with a diameter of 5 mm for a 30 cm thick sample with a 10 cm slit spacing). On the other hand, it can be seen for smaller perforation depths (5 cm) that their diameter has only a slight influence on the internal temperature of the surface, while the influence is more pronounced (0.98 ° C for a sample thickness of 10 cm) for perforations made through the entire sample (10, 20 and 30 cm). However, this influence of perforations decreases with an increase in specimen thickness (0.24 °C for a specimen thickness of 30 cm) (Figure 5). With respect to equation 12, the temperature factor fRsi also behaves in an analogous manner (Figure 6). Since the temperature factors for all combinations are greater than 0.90, the risk of surface condensation of water vapour is not affected by the performance of the perforations.

Since the coefficient of thermal coupling ($L_{3D,\ therm}$) actually reflects the total heat flow through the sample, it can be stated that the calculation results confirm expected trends (Figure 7). The decrease in $L_{3D,therm}$ with greater sample thickness and the decrease in change when the increase in thickness from 20 cm to 30 cm is compared to the increase in sample thickness from 10 cm to 20 cm. The diffusion coupling coefficient shows dependence on sample thickness (as expected), slit spacing (significant effect at lower sample thicknesses), and perforation diameter, with the results showing the somewhat surprising behaviour that 2 mm diameter perforations running throughout the sample have a minimum effect on diffusion flow of water vapour, in contrast to 5 mm diameter perforations (Figure 8).

As for the increase in heat losses, there was no significant increase if we consider a relative change with respect to the reference value of thermal conductivity of EPS, which is assumed

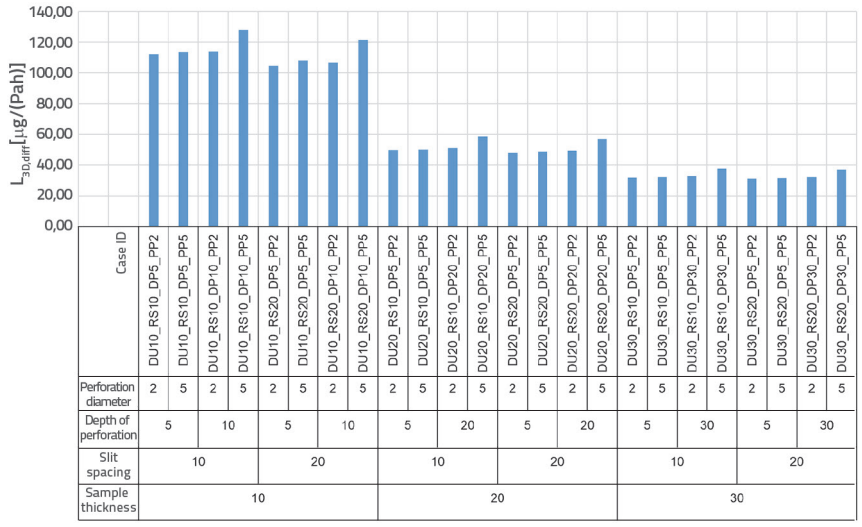

Figure 8. Diffusion coupling coefficients

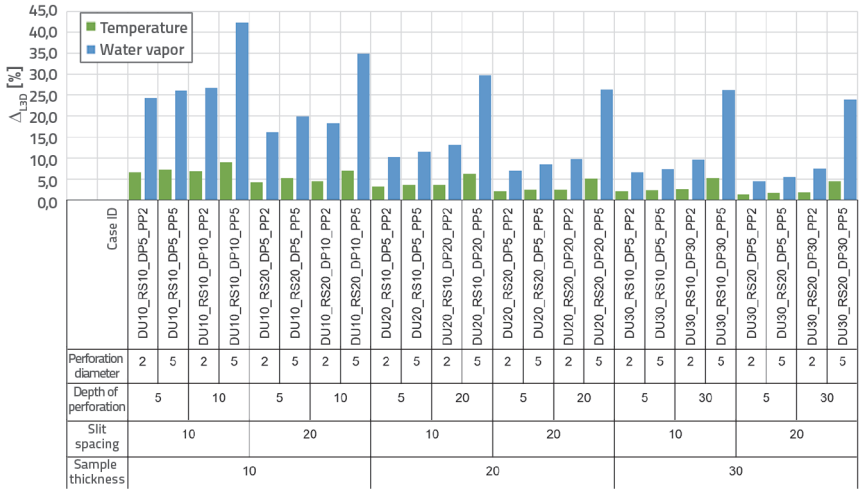

Figure 9. Comparison of the increase in heat flow and water vapour flow relative to reference cases

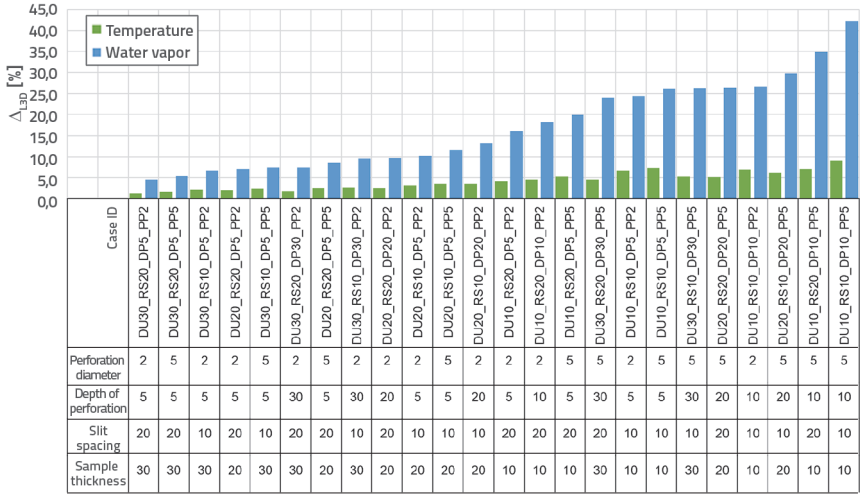

Figure 10. Comparison of increase in heat flow and water vapour flow relative to reference cases (sorted from smallest to largest).

in this work to be 0.032 W/(m K) (Figure 9 and Figure 10). This is especially true for larger sample thicknesses. The smallest and largest increase in heat loss is:

- 1.35 % for the ST30_SS20_DP5_PD2 combination.
- 9.02 % for the combination ST10_SS10_DP10_PD5.

Given the heat transfer results, the indicated minima and maxima of the diffusion flow of water vapour occurred in the expected combinations. The increase of water vapour flow occurs in the same combinations and is:

- 4.55 % for the combination ST30_SS20_DP5_PD2.
- 42.18 % for the combination ST10_SS10_DP10_PD5.

7. Effective properties of material

The effective properties of the material are calculated by deriving the effective thermal conductivity (λ_{eff}) and effective water vapour diffusion resistance (μ_{eff}) from the calculated heat flow ($L_{2D,\ therm.}$) and the effective water vapour flow ($L_{2D,\ diff}$). These effective properties of the material result in the same heat flows and water vapour diffusion flows in 1D transfer as obtained by 3D numerical calculation (Table 6).

$$\lambda_{eff} = \frac{d}{\frac{1}{2 \cdot L_{2D,therm.}} - \frac{1}{h_{si}} - \frac{1}{h_{se}}} \tag{18}$$

$$\mu_{eff} = \frac{\delta_o}{2 \cdot L_{2D,diff.} \cdot d}$$

gwhere h_{si} and h_{se} are the surface heat transfer coefficients from standard HRN EN ISO 6946 [41] (Table 5), while d is the sample thickness. The reference thermal conductivity is λ = 0,032 W/(m K), and the reference resistance to water vapour diffusion is μ = 40.

Figure 11 shows the increase in thermal conductivity compared to the reference value. Figure 12 shows the decrease in the water vapour diffusion resistance compared to the reference value, while Figure 13 presents the relative increase in thermal conductivity and the relative decrease

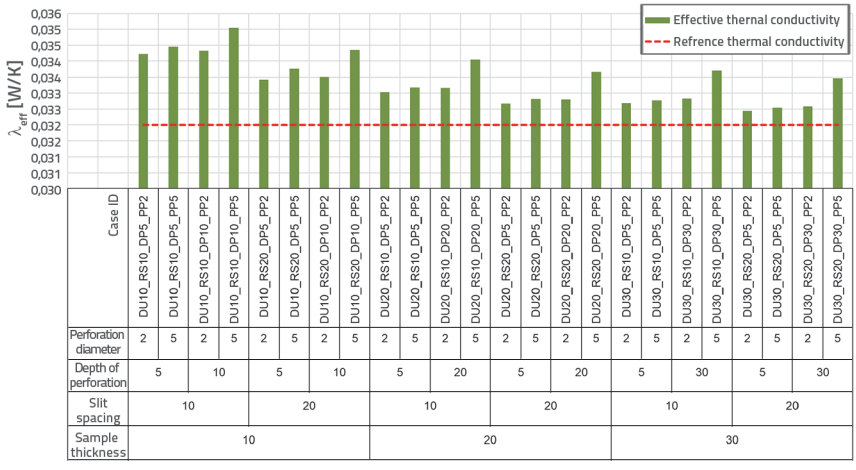

Figure 11. Effective thermal conductivity

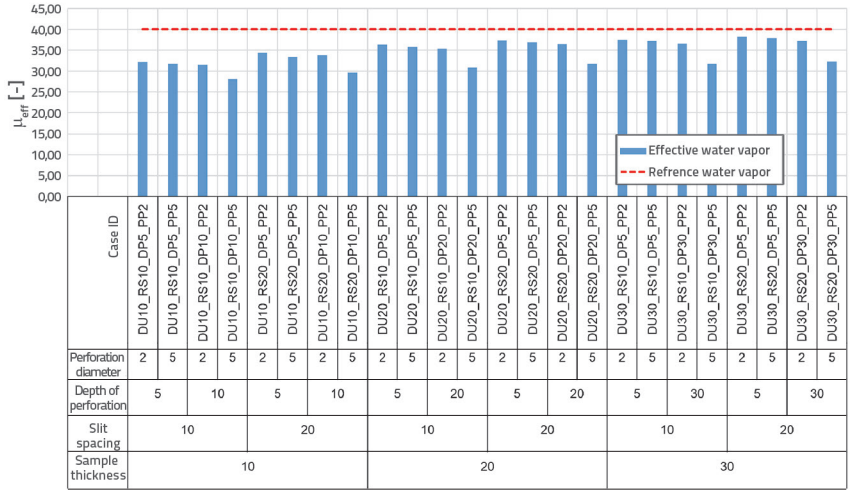

Figure 12. Effective resistance to water vapour diffusion

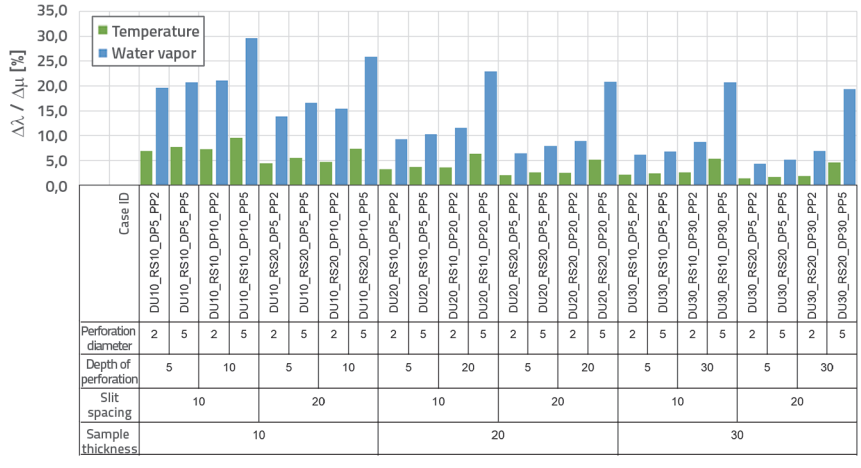

Figure 13. Increase in thermal conductivity and decrease in water vapour diffusion resistance compared to reference values

in water vapour diffusion resistance in relation to the reference values. Table 8 shows the decrease in water vapour diffusion resistance with the corresponding increase in thermal conductivity for sample thicknesses of 10, 20 and 30 cm.

Table 8. Effective material properties for sample thicknesses of 10, 20 and 30 cm

Sample thickness [cm]	μ [-]	λ [W/(m K)]	Δμ [%]	Δλ [%]
10	28.0	0.035	-29.67	+9.55
20	31.0	0.034	-22.95	+6.38
30	32.0	0.034	-20.74	+5.37

8. Conclusion

The aim of this study was to investigate the influence of perforations and slits on the change of hygrothermal properties of thermal insulation boards made of EPS, especially with regard to the change of water vapour diffusion. For these purposes, 24 different numerical models were created, and the following parameters were varied: board thickness (10, 20 and 30 cm), slit spacing (slots) (10 and 20 cm), perforation depth (5 cm and the total depth of the plate) and the diameter of the perforations (2 and 5 mm). The perforations were used to improve the water vapour diffusion properties with a minimum increase in thermal conductivity. The numerical models showed that for a board thickness of 10 cm, a slit spacing of 10 cm, a perforation depth of 10 cm, and a perforation diameter of 5 mm, up to 42.18 % better water vapour diffusion can be achieved compared to an EPS board without perforations, but with an increase in heat loss of 9.02 %. If we consider other board thicknesses, the greatest increase in water vapour diffusivity is obtained for a board thickness of:

- 20 cm (ST20_SS10_DP20_PD5): 29.79 % with an increase in thermal conductivity of 6.20 %.
- 30 cm (ST30_SS10_DP30_PD5): 26.17 % with an increase in thermal conductivity of 5.27 %.

Based on the numerical model results, it is possible to determine the effective properties of the material: the effective thermal conductivity and the effective resistance to water vapour diffusion. The maximum reduction of water vapour diffusion resistance with the corresponding increase in the coefficient of thermal conductivity for thicknesses of 10, 20 and 30 cm is as follows.

The results related to the increase in heat loss are consistent with the results of the research conducted by Molleti and van Reenan [46]. Based on 70 experiments performed on flat roofs, the authors [46] concluded that the heat flow through the flat roof system increases by 2 to 10 % depending on the thickness of the thermal insulation and the width and height of the gap between the thermal insulation boards.

It is also evident from the results of this study that the effective water vapour diffusion coefficient (μ_{eff}) depends on the sample thickness, which is in contrast to the approach usually adopted for considering this material property, where this property is assumed not to depend on the sample thickness. Here, the μ_{eff} increases with the thickness of the specimen. This means that for thicker products made of EPS, the number of perforations should be increased, or the hole diameter should be enlarged, which would consequently additionally increase the heat losses through the material.

Although this is a small increase in the thermal conductivity coefficient: from 0.032 W/(m K) to 0.035 W/(m K), the authors consider it important to emphasize that in practice this increases the thickness of thermal insulation by several centimetres. Given the efforts of manufacturers to reduce thermal conductivity with various additives (graphite) and polystyrene expanding agents, the need to reduce the vapour diffusion coefficient seems like a step backwards.

The numerical model used in this study appears to be very useful in understanding the effects of slit and perforation formation on the heat conduction and water vapour diffusion through EPS boards, and in finding the optimum perforation and slit spacing in terms of water vapour diffusion and thermal conductivity. The model itself needs further research and improvement, but the information obtained in this way will allow great savings in product development, since the production of physical samples requires development of expensive production tools, and involves additional costs for testing each product variant.

The limitations, and thus opportunities for improvement, of the numerical model used in this study can be seen in the use of steady-state methods of water vapour diffusion calculation instead of transient ones, and the modelling of independent heat and water vapour transfer instead of combined. Another opportunity for improvement is to consider the built-in moisture of the material, the ability to store and distribute moisture within the material, since moisture affects both heat and moisture transfer. In further stages of the research, the results obtained by numerical modelling will be validated by measuring the vapour transfer rate and the water vapour permeability specific to the tested sample thickness, as well as by testing the thermal conductivity using the guarded hot plate method.

Acknowledgment

The results presented in this paper are part of the research conducted within the framework of the scientific research project "Development and research of PLASTOPOR compact EPS (F) board" funded by the European Regional Development Fund (KK.01.2.1.02.0245).

REFERENCES

[1] Lakatos, Á., Kalmár, F.: Analysis of Water Sorption and Thermal Conductivity of Expanded Polystyrene Insulation Materials, Build. Serv. Eng. Res. Technol., 34 (2013), pp. 407–416, doi:10.1177/0143624412462043.

[2] Milovanović, B., Bagarić, M.: How to Achieve Nearly Zero-Energy Buildings Standard, GRADJEVINAR, 72 (2020) 8, pp. 703-720, https://doi.org/10.14256/JCE.2923.2020.

[3] Bašić, S., Vezilić Strmo, N., Marjanović, S.: Building Envelopes, GRADJEVINAR, 71 (2019) 8, pp. 673–680, https://doi.org/10.14256/JCE.1565.2016.

[4] Willems, W.M., Schild, K., Stricker, D.: Formeln Und Tabellen Bauphysik, 5. Auflage., Springer Fachmedien Wiesbaden, Wiesbaden, 2019., ISBN 978-3-658-23945-9.

[5] MPGI: Tehnički propis o racionalnoj uporabi energije i toplinskoj zaštiti u zgradama, Zagreb, NN:128/15, 70/18, 73/18, 86/18, 2020.

[6] Buczkowska, K., Pacyniak, T.: The Aging Time Effects of the Pre-Expanded Polystyrene on the Patterns Mechanical Properties, Arch. Foundry Eng., 15 (2015), pp.131–137, doi:10.1515/afe-2015-0024.

[7] Ramli Sulong, N.H., Mustapa, S.A.S., Abdul Rashid, M.K.: Application of Expanded Polystyrene (EPS) in Buildings and Constructions: A Review, J. Appl. Polym. Sci., 136 (2019), pp. 1–11, doi:10.1002/app.47529.

[8] Simpson, A., Rattigan, I., Kalavsky, E., Parr, G.: Thermal Conductivity and Conditioning of Grey Expanded Polystyrene Foams, Cellular Polymers, 39 (2020), pp. 238–262, doi:10.1177/0262489320934263.

[9] Schellenberg, J., Wallis, M.: Dependence of Thermal Properties of Expandable Polystyrene Particle Foam on Cell Size and Density, J. Cell. Plast., 46 (2010), pp. 209–222, doi:10.1177/0021955X09350803.

[10] Meftah, R., Van Stappen, J.; Berger, S., Jacqus, G., Laluet, J.-Y., Guering, P.-H., Van Hoorebeke, L.; Cnudde, V.: X-Ray Computed Tomography for Characterization of Expanded Polystyrene (EPS) Foam, Materials, (2019) 12, pp. 1–13, doi:10.3390/ma12121944.

[11] Scheirs, J., Priddy, D.B.: Modern Styrenic Polymers: Polystyrenes and Styrenic Copolymers, John Wiley & Sons Ltd., 2003.

[12] National Research Council et al.: Review of the Styrene Assessment in the National Toxicology Program 12th Report on Carcinogens, Workshop Summary, Washington (DC), 2014.

[13] Bjegović, D., Banjad Pečur, I., Milovanović, B., Jelčić Rukavina, M., Alagušić, M.: Usporedba ponašanja različitih ETICS sustava u uvjetima požara ispitivanjem u stvarnoj veličini, Građevinar, 68 (2016) 5, pp. 357–369, doi:10.14256/JCE.1347.2015.

[14] Eder, C.: GEG-Baupraxis, Bauteilen, 2014., pp. 9

[15] Tatara, J., Ricketts, L.: Impact of Heating and Cooling of Expanded Polystyrene and Stone Wool Insulations on Conventional Roof Performance, Proceedings of the 15th Canadian Conference on Building Science and Technology; British Columbia Building Envelope Council, Vancouver, Canada, 2017., pp. 1–16

[16] Blazejczyk, A., Jastrzebski, C., Wierzbicki, M.: Change in Conductive–Radiative Heat Transfer Mechanism Forced by Graphite Microfiller in Expanded Polystyrene Thermal Insulation—Experimental and Simulated Investigations, Materials, 13 (2020), pp. 2626, doi:10.3390/ma13112626.

[17] Ademović, Z., Suljagić, J., Zulić, J.: Influence of Physical Properties on Thermal Conductivity of Polystyrene Insulation Materials, Contemp. Mater., 8 (2017), pp. 42–47, doi:10.7251/COMEN1701042A.

[18] Rockwool North America: Dimensional Stability on the Roof, https://www.rockwool.com/north-america/advice-and-inspiration/learning/advice/dimensional-stability-on-the-roof/, 17.1.2021.

[19] Palmer, J.: Annex 19: Low Slope Roof Systems, Birmingham, 2003.

[20] Hens, H.: Performance Based Building - Design 1, 2nd Edition, Wiley-VCH Verlag GmbH & Co. KGaA, Weinheim, Germany, 2012., ISBN 9783433601952.

[21] Vimark: EPS Sheets with Graphite for Thermal Insulation Systems, https://www.vimark.com/wp-content/uploads/2015/09/COVER_GRAFITE_80_0116_ENG.pdf, 2016.

[22] BASF: Neopor Professional Brochure, https://neopor.de/portal/load/fid1225157/Neopor_professional%20brochure.pdf, 2014.

[23] Endres, E., Kleser, J.: Wärmedämmstoffe aus Polyurethan-Hartschaum Herstellung, https://daemmtbesser.de/fileadmin/user_upload/IVPU_Fachbroschuere_200903_Waermedaemstoffe_aus__PU-Hartschaum.pdf, 2008.

[24] Hrvatski Zavod za norme: HRN EN 12086, Toplinsko-izolacijski proizvodi za graditeljstvo – određivanje paropropusnosti, 2013.

[25] Mánik, M., Medved, I.: Transmission of Water Vapor through Expanded Polystyrene, Proceedings of the Central European Symposium on Thermophysics 2020 (CEST 2020), AIP Publishing, Olomouc, Czech Republic, 2020., pp. 020020-1-020020–020026

[26] Koch, M.: Thermal Insulation Panels Made of EPS or PUR Have an Array of Perforations to Increase Their Water Vapor Permeability, https://patents.google.com/patent/DE10007774A1/en, 2001.

[27] Weier, A., Schnelle, R., Kohler, E.: Patent Offenlegungsschrift, 2010, pp. 8

[28] Lassen, C., Maag, J., Hoibye, L.. Verterlykke, M., Lundegaard, T.: Alternatives to the use of flame retarded EPS in buildings, Climate and Pollution Agency, Oslo, 2011.

[29] WDVS: Bauexpert, https://www.bauexpert.it/fileadmin/user_upload/Webbilder_Kunde/01_bauexpert/03_downloads/katalog/de_bauexpert_wdvs_2014.pdf ,2014., pp. 80

[30] EPS-Industries: Sympor Baustoffhandel, https://www.eps-industries.at/images/produkte/Baustoffkatalog.pdf, 2019, pp. 33

[31] Rofix: EPS-F-031-Relax,Tehnički list, 2021.

[32] Brucha: Wärmedämmplatte EPS-F Klima, katalog, 2016.

[33] Baumit: OpenTherm 032 G, katalog, 2020.

[34] Baumit: Fasadna Ploča Openair, katalog, 2017.

[35] Landolfi, R., Nicolella, M.: Durability Assessment of ETICS: Comparative Evaluation of Different Insulating Materials, Sustainability, 14 (2022), pp. 1–25, doi:10.3390/su14020980.

[36] American Society of Heating, Refrigerating and Air-Conditioning Engineers: RP-1018 Thermal & Moisture Transport, Database For Common BLDG & Insulating Materials, 2002, pp. 229

[37] Ducoulombier, L.; Lafhaj, Z.: Comparative Study of Hygrothermal Properties of Five Thermal Insulation Materials, Case Stud. Therm. Eng., 10 (2017), pp. 628–640, doi:10.1016/j.csite.2017.11.005.

[38] Künzel, H., Wieleba, R.: Specific Building-Physical Properties of ETICS on Mineral-Wool Basis, 2009.

[39] Hrvatski Zavod za norme: HRN EN ISO 10211:2017- Toplinski mostovi u zgradarstvu: toplinski tokovi i površinske temperature - detaljni proračuni, ISO 10211:2017; EN ISO 10211:2017, 2017., pp. 60

[40] Hrvatski Zavod za norme: HRN EN ISO 13788:2002 - Značajke građevnih dijelova i građevnih dijelova zgrada s obzirom na toplinu i vlagu; temperatura unutarnje površine kojom se izbjegava kritična vlažnost površine i unutarnja kondenzacija; metode proračuna, ISO 13788:2001; EN ISO 13788:2001, 2002., pp. 37

[41] Hrvatski Zavod za norme: HRN EN ISO 6946:2017: Građevni dijelovi i građevni elementi; toplinski otpor i koeficijent prolaska topline; metode proračuna, ISO 6946:2017; EN ISO 6946:2017, 2017., pp. 45

[42] Hrvatski Zavod za norme: HRN EN ISO 10077-2:2017: Toplinska svojstva prozora, vrata i zaslona - Proračun koeficijenta prolaska topline, 2. dio: Numerička metoda za okvire, ISO 10077-2:2017; EN ISO 10077-2:2017, 2017., pp. 75

[43] Kornicki: Dienstleistungen in EDV und Informationstechnologie, AnTherm, Wien, 2020.

[44] Hens, H.: Building Physics Heat, Air and Moisture Fundamentals and Engineering Methods with Examples and Exercises, 2nd Edition, Wilhelm Ernst & Sohn, 2012.; ISBN 9783433030271.

[45] Kreč, K.: Notiz Zu Den von AnTherm Verwendeten Berechnungsgrundlagen Zur Beschreibung Mehrdimensional Ablaufender Wasserdampf-Diffusionsvorgänge, http://hilfe.antherm.eu/Theory/Notiz_Diffusion.pdf , 5.6.2021.

[46] Molleti, S., van Reenen, D.: Development of Psi Factors for Thermal Bypass Due to Insulation Gaps in Low-Slope Roofing Assemblies, Buildings, 12 (2022), pp. 16, doi:10.3390/buildings12010068.